Complex of Human Apolipoprotein C-1 with Phospholipid: Thermodynamic or Kinetic Stability?†

Olga Gursky,* Ranjana, and Donald L. Gantz

Department of Physiology and Biophysics, Boston University School of Medicine, 715 Albany Street, Boston, Massachusetts 02118

Received January 24, 2002; Revised Manuscript Received March 8, 2002

ABSTRACT: Thermal unfolding of discoidal complexes of apolipoprotein (apo) C-1 with dimyristoyl phosphatidylcholine (DMPC) reveals a novel mechanism of lipoprotein stabilization that is based on kinetics rather than thermodynamics. Far-UV CD melting curves recorded at several heating/cooling rates from 0.047 to 1.34 K/min show hysteresis and scan rate dependence characteristic of slow nonequilibrium transitions. At slow heating rates, the apoC-1 unfolding in the complexes starts just above 25 °C and has an apparent melting temperature $T_m \sim 48 \pm 1.5$ °C, close to $T_m = 51 \pm 1.5$ °C of free protein. Thus, DMPC binding may not substantially increase the low apparent thermodynamic stability of apoC-1, ΔG(25 °C) < 2 kcal/mol. The scan rate dependence of T_m and Arrhenius analysis of the kinetic data suggest an activation enthalpy $E_a = 25 \pm 5$ kcal/mol that provides the major contribution to the free energy barrier for the protein unfolding on the disk, $\Delta G^* \geq 17$ kcal/mol. Consequently, apoC-1/DMPC disks are kinetically but not thermodynamically stable. To explore the origins of this kinetic stability, we utilized dynode voltage measured in CD experiments that shows temperature-dependent contribution from UV light scattering of apoC-1/DMPC complexes ($d \sim 20$ nm). Correlation of CD and dynode voltage melting curves recorded at 222 nm indicates close coupling between protein unfolding and an increase in the complex size and/or lamellar structure, suggesting that the enthalpic barrier arises from transient disruption of lipid packing interactions upon disk-to-vesicle fusion. We hypothesize that a kinetic mechanism may provide a general strategy for lipoprotein stabilization that facilitates complex stability and compositional variability in the absence of high packing specificity.

Lipoproteins are heterogeneous macromolecular complexes of variable protein and lipid composition, size, density, and metabolic properties (reviewed in refs *1*−*4*). Abnormal plasma levels of lipoproteins are associated with several major human diseases, most commonly atherosclerosis. The probability of developing atherosclerosis correlates with the balance between the low-density lipoproteins (LDL)[1] that mediate cholesterol delivery and high-density lipoproteins (HDL) that mediate cholesterol removal. Nascent HDL form phospholipid bilayer disks containing cholesterol and specific proteins (termed apolipoproteins) that are wrapped around the disk circumference and thereby screen the phospholipid acyl chains from the aqueous milieu. Mature lipoproteins, that are converted to spheres by the action of lecithin: cholesterol acyltransferase (LCAT), acquire an apolar core of cholesterol ester and triglycerides. Exchangeable, or water-soluble, apolipoproteins transfer among plasma lipoproteins, thereby imparting to them such metabolic properties as activation of LCAT or other enzymes regulating lipid metabolism, LDL or HDL receptor binding activity, or stimulation of cellular cholesterol efflux. In the course of their metabolism, lipoproteins undergo extensive changes in protein and lipid composition, size, and shape, yet they possess sufficient structural stability to carry out their functions. Reduced lipoprotein stability is linked to abnormal lipid metabolism in such diseases as hypertriglyceridemia (*5*). Thus, the mechanism of lipoprotein stability is key to understanding lipoprotein action in normal and in diseased states, and is in the focus of this work.

In the lipid-free state in solution, the exchangeable apolipoproteins have marginal thermodynamic stability, ΔG(25 °C) ≤ 2.4 kcal/mol (*6*), and exhibit other properties of the molten globule state (such as compact shape with high α-helix content but lack of specific tertiary interactions, broad thermal unfolding, affinity for various hydrophobic ligands, etc.) that may mediate protein−lipid interactions (*7*, *8*, reviewed in ref *9*). Apolipoproteins can associate with phospholipids in vitro, forming discoidal complexes that model the physicochemical and functional properties of nascent HDL (*2*, *10*). Complex formation with phospholipids is accompanied by protein conformational changes that involve an increase in the α-helical content (*9*, *11*). The

† This work was supported by the National Institute of Health Grant HL61429 to O.G.; support for CD spectroscopy and electron microscopy comes from the NIH Program Project Grant HL26355 (D. Atkinson, P.I.).

* Corresponding author: Olga Gursky. E-mail: Gursky@biophysics.bumc.bu.edu. Phone: (617) 638-7894. Fax: (617) 638-4041. Address: Department of Physiology and Biophysics, W329, Boston University School of Medicine, 715 Albany St., Boston, MA 02118.

[1] Abbreviations: Apo, apolipoprotein; HDL, high-density lipoprotein; LDL, low-density lipoprotein; DMPC, dimyristoyl phosphatidylcholine; PC, phosphatidylcholine; LCAT, lecithin:cholesterol acyltransferase; CD, circular dichroism; DSC, differential scanning calorimetry.

10.1021/bi025588w CCC: $22.00
Published on Web 05/15/2002

largest increase, from 31% up to 75% α-helix, is observed in apolipoprotein C-1 (apoC-1, 57 aa) (*12* and references therein), the smallest human apolipoprotein that transfers between HDL and VLDL. ApoC-1 is characterized by high sequence homology, structural and functional similarity to larger members of this protein family (*11*−*16*), providing an attractive model for an energetic and structural analysis of the lipid-free (*17*, *18*) and lipid-bound apolipoproteins. In this work, we analyze the thermal stability of discoidal complexes of apoC-1 and dimyristoyl phosphatidylcholine (DMPC). Such reconstituted lipoproteins may model the stability properties of nascent HDL that also have phosphatidylcholines (PCs) as their major lipid constituents.

Complex formation with phospholipids is reported to stabilize apolipoproteins against proteolysis as well as chemical and thermal unfolding (for recent references see refs *19* and *20*). This stabilization is usually expressed in terms of changes in the free energy difference $\Delta G = G_U - G_F$ between the unfolded and folded protein states (*5*, *20*−*22* and references therein), that is an equilibrium thermodynamic potential. However, the applicability of equilibrium thermodynamics to lipoproteins has been questioned by the irreversibility of their unfolding that was observed by Reijngoud and Phillips in spectroscopic studies of chemical denaturation of apoA-1/DMPC complexes (*23*), and was suggested by thermal unfolding and refolding studies of these and other reconstituted lipoproteins by differential scanning calorimetry (DSC) (*24*−*26*). These and most other thermal unfolding data on lipoproteins were recorded at a single scanning rate (typically ≥ 60 K/h) and thus were insufficient to test the equilibrium character of the transition. The exception is the work of Epand and colleagues that revealed a marked heating rate dependence in the calorimetric transition of apoA-1/DMPC complexes recorded at 10 and 90 K/h; this observation, along with kinetic data recorded by spectroscopy, indicated slow nonequilibrium unfolding and suggested that the complex stability is determined by kinetic factors (*27*, *28*).

Here, we use circular dichroism (CD) along with fluorescence spectroscopy and electron microscopy to carry out a comprehensive analysis of the thermal unfolding in discoidal apoC-1/DMPC complexes that allows us to unambiguously differentiate between the thermodynamic and kinetic mechanisms of their stabilization. We also use the CD spectrometer to detect heat-induced changes in UV light scattering of apoC-1/DMPC complexes and correlate them with the protein unfolding, thereby providing a clearer insight into the physical origins of lipoprotein stability. Our results challenge the existing paradigm of lipoprotein stabilization and may have important functional implications.

MATERIALS AND METHODS

Sample Preparation. Full-size human apoC-1 (57 aa) was obtained by solid-state synthesis and purified by HPLC to 98% purity as described (*18*); the peptide termini were not chemically blocked. Lyophilized peptides were dissolved to 1 mg/mL concentration and diluted by buffer (5 mM sodium phosphate, pH 7.8) to 5−100 μg/mL for spectroscopic experiments. Synthetic lipid-free apoC-1 prepared by this method has secondary structure and stability properties similar to those of human plasma apoC-1 (*18*). ApoC-1/DMPC complexes were prepared using protein-to-lipid ratio of 1:5 mg/mg. Protein solution of 0.1 mg/mL concentration was added to the suspension of DMPC liposomes and incubated at room temperature, i.e., near the temperature of the gel-to-liquid crystalline transition of DMPC, $T_c \sim 24$ °C, at which the protein−lipid association is fastest. The mixture cleared within 1 h of incubation; after overnight incubation, the samples were diluted by buffer to the final protein concentration ranging from 5 to 100 μg/mL and were used for spectroscopic and electron microscopic studies. All chemicals were highest purity analytical grade.

Electron Microscopy of ApoC-1/DMPC Complexes. ApoC-1/DMPC complexes were imaged using the negative staining technique (*29*). A 4 μL aliquot was incubated for 1 min on a carbon, Formvar-coated 300 mesh copper grid. After blotting excess fluid, the sample was stained with 1% sodium phosphotungstate at pH 7.4, blotted, and air-dried. Images were recorded under low-dose conditions on SO163 film in a CM12 transmission electron microscope (Philips Electron Optics, Eindhoven, Netherlands). Films were developed in D19 and scanned on an EverSmart Supreme Scanner (CreoScitex Corp., Vancouver, Canada). Images were cropped and processed in Scion Image (Scion Corp., Frederick, MD). Statistical analysis of the disk size distribution was carried out using EXCEL program; such an analysis has higher resolution and yields more accurate disk size estimates than alternative techniques such as nondenaturing gel electrophoresis. All electron microscopic experiments were carried out in quadruplicate to ensure reproducibility.

Circular Dichroism Spectroscopy. CD signal, dynode voltage, and sample temperature were recorded with an AVIV 62-DS spectrophotometer equipped with thermoelectric temperature control and calibrated with d_{10}-camphorosulfonic acid. Far-UV CD spectra (185−250 nm), thermal unfolding, and kinetic data were recorded from solutions of 7−20 μg/mL protein concentrations placed in 5−10 mm quartz cells; near-UV CD spectra (250−330 nm) were recorded from 0.1 mg/mL protein solutions in 10-mm cells. The spectra were recorded with 1-nm bandwidth, 1-nm increment, 15 s accumulation time, and averaged over three scans. Thermal unfolding and refolding data at 222 nm were recorded upon sample heating and cooling from 25 to 85 °C, with 1 °C increment, 30−300 s accumulation time per data point, 0−600 s equilibration time at each temperature. Actual scan rates determined by careful timing of the heating and cooling experiments ranged from 0.047 to 1.34 K/min. Kinetic experiments were carried out at 222 and 193 nm by following the time course of the protein unfolding or refolding resulting from the abrupt temperature changes in the range from 25 to 85 °C; the sample temperature reached equilibrium within <2 min after the T-jump. All experiments were repeated 3−4 times; the CD spectra, melting and kinetic data recorded in such repetitive experiments closely superimposed.

Following the buffer baseline subtraction, the CD data were normalized to protein concentration and are reported as molar residue ellipticity, [Θ]. Normalized CD data were independent of the apoC-1/DMPC disk concentrations in the range explored. Protein α-helical content was estimated as described (*18*). The apparent melting temperature T_m was determined from differential melting curves $d[\Theta_{222}](T)/dT$ (*30*). Prior to differentiation, the melting curves $[\Theta_{222}](T)$ were smoothed by a third degree polynomial or by using a

Fourier transform-based algorithm, which did not affect the peak position T_m in d[Θ_{222}](T)/dT function. ORIGIN software was used for the data analysis and display.

Fluorescence Spectroscopy. Fluorescence measurements were facilitated by the presence of one Trp (W41) and no Tyr in the apoC-1 sequence. Intrinsic Trp fluorescence spectra were recorded at 25 °C using FluoroMax-2 spectrofluorimeter with water bath temperature control. Fresh samples containing filtered buffer and/or free apoC-1 or apoC-1/DMPC complexes were placed in 1-cm square cells. The emission spectra were recorded at 310−400 nm using the excitation wavelength 290 nm; the buffer spectra were subtracted. The spectral shapes and relative intensities were invariant with changes in the protein concentration from 5 to 20 μg/mL, indicating the absence of a significant inner filter effect. Fluorescence spectra recorded in repetitive experiments were highly reproducible.

Kinetic Analysis. Thermal transition of apoC-1/DMPC disks was analyzed by using a simple first-order Arrhenius model. For a first-order unfolding reaction:

$$\mathrm{d[C]/dt} = -k[\mathrm{C}] \quad (1)$$

Here [C] is the concentration of the folded species, and k is the temperature-dependent reaction rate. The rate constant k follows an Arrhenius law if

$$k(T) = A \exp(-E_a/RT) \quad (2)$$

Here, A is temperature-independent rate constant in the absence of the kinetic barrier E_a, $R = 1.987$ kcal/mol is universal gas constant, and T is absolute temperature. If $E_a(T) = \text{const}$, the Arrhenius plot ln(k) versus $1/T$ is linear with a slope $-E_a/R$. The value of E_a for the apoC-1/DMPC disk transition was estimated from the slope of such a plot. The transition rates k at several temperatures from 40 to 85 °C were determined as $k = 1/\tau$, where τ is exponential relaxation time obtained from single-exponential fitting of the kinetic data $\Theta_{222}(t)$.

In addition, the energy barrier E_a for the apoC-1/DMPC disks transition was determined from the heating rate dependence of the apparent melting temperature T_m. For a thermodynamically irreversible transition that can be described by the Lumry-Eyring model and obeys the Arrhenius law, the effect of the scanning rate υ on T_m can be expressed as (*31*, *32*)

$$\ln(\upsilon/T_m^2) = \text{const} - E_a/RT_m \quad (3)$$

If the energy barrier $E_a(T) = \text{const}$, the plot ln(υ/T_m^2) versus $1/T_m$ is linear with a slope $-E_a/R$. The value of E_a for the apoC-1 unfolding on DMPC disks was determined from such a plot, with the values of T_m obtained from the first derivative functions d[Θ_{222}](T)/dT of the CD melting curves $\Theta_{222}(T)$ recorded at several heating rates υ from 0.047 to 1.34 K/min.

The activation Gibbs free energy ΔG^* is related to the reaction rate k via the Eyring equation (*33*, *34*):

$$k = (k_B T/h) \exp(-\Delta G^*/RT) \quad (4)$$

Here $k_B = 1.38 \times 10^{-23}$ J/K is the Boltzmann constant, $h = 6.63 \times 10^{-34}$ J s is the Plank constant, and R is universal gas constant. Application of the Eyring equation to protein folding is associated with the uncertainty in the preexponential factor. In the temperature range of protein unfolding, the prefactor $k_B T/h = 6-7 \times 10^{12}$ s^{-1} is substantially higher than the fastest rates observed for protein folding/unfolding that fall in the milli-to-nanosecond range (*35* and references therein). Therefore, the prefactor for the unfolding of small proteins and peptides is usually assumed to be 10^7-10^8 s^{-1} (*36*, *37*). Using this assumption and the reaction rates determined from the kinetic data recorded in temperature-jump (T-jump) experiments from 25 to 40−85 °C, we estimated the free energy barrier ΔG^* for the apoC-1 unfolding on DMPC disks.

RESULTS

Electron Microscopy of ApoC-1/DMPC Complexes. The morphology of the apoC-1/DMPC complexes prepared at 25 °C and subjected to various thermal treatments was observed by negative staining electron microscopy (Figure 1). Figure 1A shows an electron micrograph of a freshly prepared sample at 25 °C. The predominant species are apoC-1/DMPC disks that are seen in a "face-up" orientation or stacked on edge in rouleaux; such stacks are unique to negative staining preparations and facilitate accurate disk size determination (*38*). The disk thickness estimated from the rouleaux is 5.56 ± 0.10 nm, which is the thickness of the DMPC bilayer; the disk diameters range from about 15−20 nm, with an average $\langle d \rangle = 16.9 \pm 2.7$ nm. Such a diameter corresponds to the protein/lipid ratio of about 1:4.7, close to that used for the sample preparation. Consequently, most of the material in apoC-1/DMPC samples is present in discoidal complexes.

Figure 1B shows that equilibration of a similar sample for 12 h at 40 °C followed by a 20 min equilibration at 25 °C leads to an increase in the disk diameter to $\langle d \rangle = 30.4 \pm 6.4$ nm without altering its thickness. Figure 1C shows that equilibration of a similar sample for 1 h at 65 °C followed by 20 min equilibration at 25 °C results in a diameter increase to $\langle d \rangle = 31.3 \pm 6.4$ nm. The equilibration times in these experiments (selected based on the results of the kinetic CD studies depicted in Figures 5 and 6) ensure that the temperature-induced conformational changes in the protein moiety reach a steady state. Figure 1D shows a similar sample that was consecutively heated and cooled from 25 to 85 °C at a rate 0.047 K/min, followed by incubation at 25 °C for 1 week. Compared to a fresh disk solution (Figure 1A), the average disk diameter shows a small increase to $\langle d \rangle = 21.6 \pm 1.4$ nm ($p < 0.05$). Thus, even after prolonged incubation at 25 °C, the heat-induced changes in apoC-1/DMPC disks may not be fully reversible.

Effect of DMPC Binding on the Secondary Structure and Thermal Unfolding of ApoC-1. Far-UV CD spectra of apoC-1/DMPC complexes recorded at 25 and 75 °C are shown in Figure 2. The spectra at 25 °C (Figure 2A) indicate that the apoC-1/DMPC disk formation is accompanied by a large increase in the protein α-helix content, from 31 to ∼75%, similar to that observed in plasma apoC-1 (*12*). The spectra recorded after 1 h equilibration at 75 °C (Figure 2B), that is, in the post-transitional region of the heat unfolding (see Figures 3A and 4A), show more negative CD amplitude for the apoC-1/DMPC complexes as compared to free protein. This increase in CD cannot be an artifact of absorption

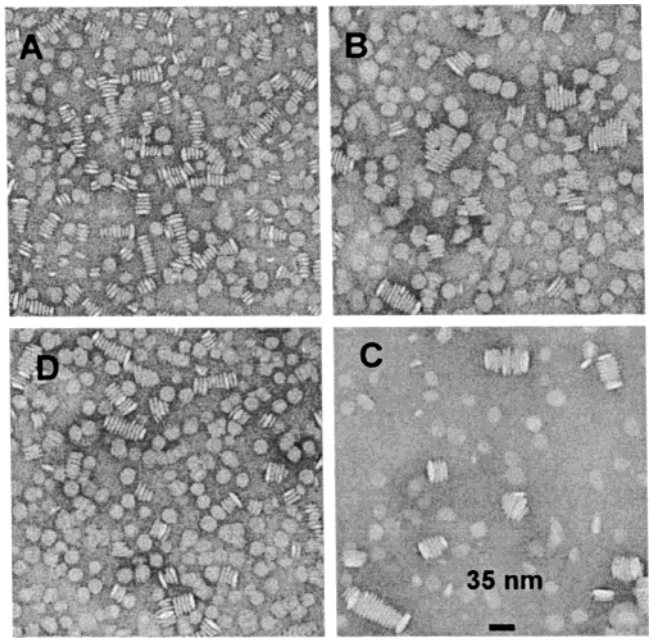

FIGURE 1: Negative staining electron micrographs of apoC-1/DMPC disks subjected to various thermal treatments. Protein concentration is 10 μg/mL, protein/lipid ratio is 1:5 mg/mg. (A) Freshly prepared sample (after overnight incubation at 25 °C); (B) similar sample after 12 h equilibration at 40 °C followed by 20 min equilibration at 25 °C; (C) similar sample after 1 h equilibration at 65 °C followed by 20 min equilibration at 25 °C; (D) similar sample after heating and cooling from 25 to 85 °C at a rate υ = 0.047 K/min followed by 1 week incubation at 25 °C.

flattening [that leads to a reduction rather that an increase in the CD signal measured from suspensions of large particles with high protein concentrations (*39*)] or differential light scattering [that is shown to be insignificant in the CD spectra of comparable size particles with $d \sim 25$ nm (*39*)]. Therefore, higher CD amplitude of apoC-1/DMPC samples observed at 75 °C must result from higher helical content retained by apoC-1 in these samples as compared to free protein. This suggests that the melting of apoC-1/DMPC disks does not lead to complete protein dissociation from the lipid. Thus, similar to apoA-1 that was found on vesicular complexes with PCs (*10* and references therein), apoC-1 at high temperatures may remain partially associated with the lipid.

Thermal unfolding and refolding of the helical structure in free apoC-1 and in apoC-1/DMPC disks was monitored by CD at 222 nm. The $[\Theta_{222}](T)$ data recorded during heating from 25 to 85 °C followed by cooling to 25 °C at a rate υ = 1.34 K/min (~80 K/h) are shown in Figure 3. The unfolding and refolding curves of lipid-free protein largely overlap (Figure 3A), and the ellipticity at 222 nm and other wavelengths after heating and cooling from 25 to 85 °C is restored to ≥ 95% of its original value. The ≤5% loss in the CD signal is typical of protein heat unfolding (*40*) and can be accounted for by protein aggregation and/or absorption to the cell walls at high temperatures (T > 70 °C); indeed, far-UV CD spectra of free apoC-1 monomer recorded at 25 °C before and after heating to 65 °C fully overlap, indicating complete reversibility of the transition (data not shown). The melting curve of free apoC-1 can be approximated by a single sigmoidal function (Figure 3A, solid line). The midpoint of this function coincides with the temperature at which 50% of the total CD changes are observed, $T_{1/2} = 51 \pm 1.5$ °C, and with the peak position in the first derivative function $d[\Theta_{222}]/dT$, $T_m = 51 \pm 1$ °C (Figure 3A, inset). Furthermore, the $[\Theta_{222}](T)$ data recorded at different scan rates from about 0.1−1.3 K/min fully overlap. These observations indicate equilibrium character of the transition (*31*).

In contrast to free protein unfolding, thermal transition of apoC-1/DMPC complexes displays hysteresis. At υ = 1.34 K/min, the refolding data are shifted by about −35 °C compared to the unfolding data (Figure 3B), suggesting a shift in the population distribution toward the preexisting species and implicating the presence of a kinetic barrier separating these species. The unfolding curve of apoC-1 on DMPC is sharper at high temperatures and thus cannot be fitted by a single sigmoidal function. This is reflected in the discrepancy between $T_{1/2} = 66 \pm 1.5$ °C and $T_m = 72 \pm 1$ °C and in the asymmetry of the first derivative peak $d[\Theta_{222}]/dT$ (Figure 3B, inset), which is another indicator of the nonequilibrium unfolding (*31*). In addition, heating and cooling from 25 to 85 °C results in nearly 17% loss in the CD signal at 222 nm (Figure 3B) and other wavelengths, suggesting partial irreversibility of the apoC-1 unfolding on DMPC disks.

Scan Rate Effects on the Thermal Transitions of ApoC-1/DMPC Complexes. To test whether the unfolding of the protein moiety in apoC-1/DMPC complexes can be recorded under equilibrium conditions at slower scan rates, the α-helical content in these complexes was monitored by CD at 222 nm during heating and cooling from 25 to 85 °C at several constant rates ranging from 1.34 to 0.047 K/min (i.e., from about 80 to 2.8 K/h) (Figure 4). In contrast to free protein unfolding, the melting curves of apoC-1/DMPC complexes show strong scan rate dependence that is markedly different for the heating and cooling curves (Figure 4A). Heat unfolding curves of apoC-1 on DMPC complexes show progressive low-temperature shifts upon reduction in the heating rate from 1.34 to 0.047 K/min that correspond to a reduction in $T_{1/2}$ from 66 to 48 °C and in T_m from 72 to 48 °C (Figure 4A,B). Reducing the scan rate also leads to an increased symmetry in $[\Theta_{222}](T)$ and $d[\Theta_{222}](T)/dT$ curves (Figure 4A,B) and thus to a better agreement between T_m and $T_{1/2}$ ($T_m = T_{1/2}$ at $\upsilon \leq 0.1$ K/min). At heating rates below 0.05 K/min, no further changes in T_m are observed. Remarkably, the apparent melting temperature of apoC-1/DMPC complexes observed in slow heating experiments ($\upsilon \leq 0.05$ K/min, open triangles in Figure 4A), $T_{m,C1:DMPC} = 48 \pm 1.5$ °C, is comparable to that of lipid-free apoC-1, $T_{m,C1} = 51 \pm 1.5$ °C (Figure 3A). Furthermore, similar to the unfolding of free apoC-1, slow heating of apoC-1/DMPC disks leads to protein unfolding that starts just above 25 °C and becomes significant at 37 °C where nearly 10% of the total change in the CD amplitude Θ_{222} is observed (Figure 3A, Figure 4A, open triangles). Therefore, similar to free apoC-1, the apoC-1/DMPC disks have only marginal thermodynamic stability at these temperatures.

In contrast to the heat unfolding curves, the refolding curves recorded at several relatively fast cooling rates fully overlap (υ = 0.76−1.34 K/min, closed symbols in Figure 4A), suggesting relatively fast refolding kinetics. Surprisingly, increased deviations among the refolding curves are observed at slower cooling rates (υ < 0.76 K/min, open symbols in Figure 4A), suggesting that the protein refolding

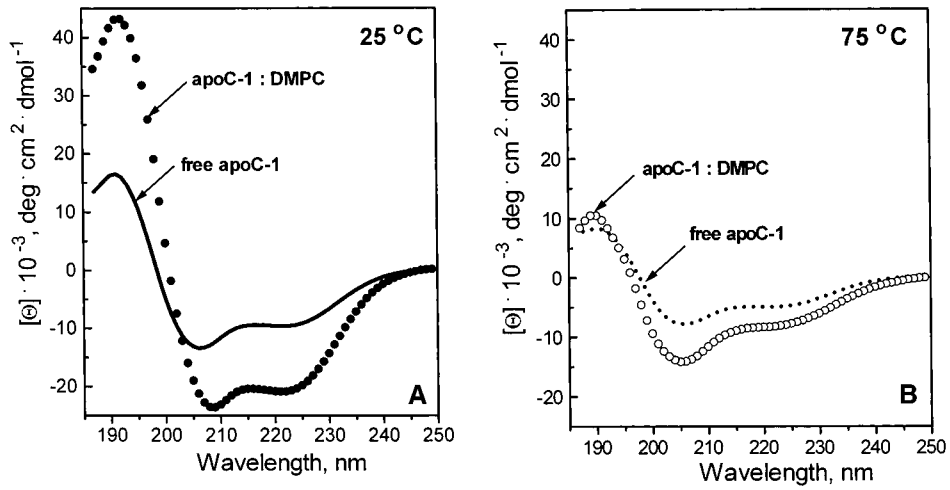

FIGURE 2: Far-UV CD spectra of apoC-1/DMPC complexes as compared to free apoC-1 monomer. All samples contain 10 μg/mL protein in 5 mM sodium phosphate buffer (pH 7.8), apoC-1/DMPC ratio is 1:5 mg/mg; samples were prepared at 25 °C and equilibrated overnight at 25 °C prior to the CD data collection. Solid or dotted lines show spectra of free protein, circles show spectra of apoC-1/DMPC complexes. The spectra were recorded after sample equilibration at 25 °C (A) and 75 °C (B).

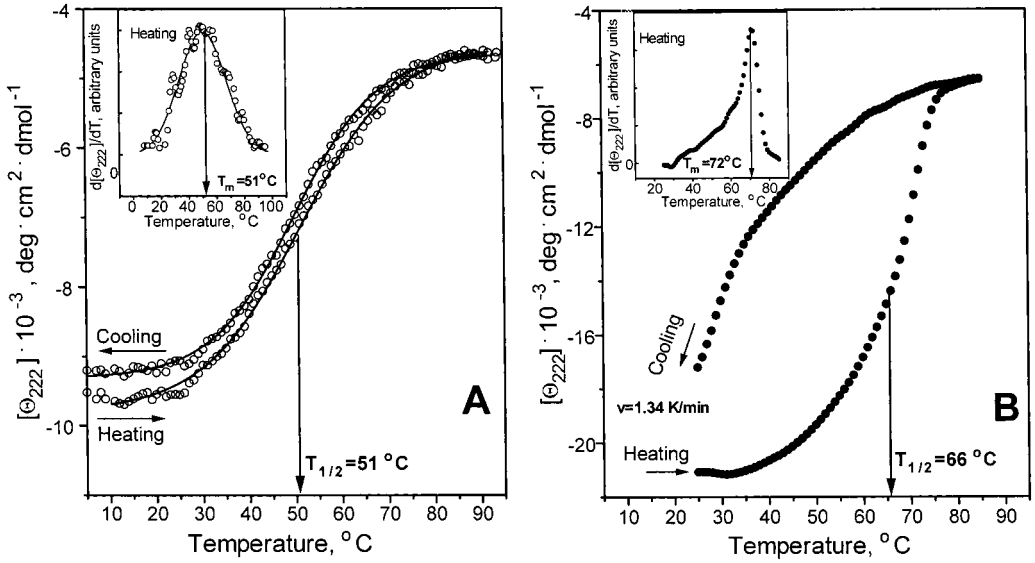

FIGURE 3: Thermal unfolding and refolding of apoC-1 in complex with DMPC and in monomeric lipid-free state. Protein helical content was monitored by CD at 222 nm upon heating and cooling at a rate $\upsilon = 1.34$ K/min. Sample conditions are same as in Figure 2. (A) Free apoC-1 monomer (○); (B) apoC-1/DMPC complexes (●). Arrows indicate apparent midpoint temperatures $T_{1/2}$ of the heat unfolding transitions. Insets: First derivative functions $d\Theta_{222}/dT$ of the heat unfolding data. Apparent melting temperatures T_m corresponding to the maximum in $d\Theta_{222}/dT$ functions are shown by arrows. The reproducibility in the T_m values obtained in different experiments under identical conditions is better than 2 °C.

on DMPC complexes is a complex nonequilibrium transition. Indeed, if equilibrium could be attained, then upon lowering the scan rate the unfolding and refolding curves would shift toward each other and eventually overlap. This contrasts with the observed cooling rate dependence in the refolding curves (such as low- rather than high-temperature shifts at slow cooling rates resulting in the hysteresis at any scan rate explored), suggesting complex kinetics of the disk reconstitution upon cooling from high temperatures and indicating nonequilibrium character of the transition at any scan rate.

Rate of ApoC-1 Folding/Unfolding on DMPC Disks. The kinetics of thermal transitions in apoC-1/DMPC disks was probed by following the time course of the protein unfolding and refolding on the disk in T-jump experiments (*41* and references therein). In one such experiment, the temperature of apoC-1/DMPC disk solution was rapidly raised from 25 to 45 °C (that is close to the apparent $T_m \sim 48$ °C of the disks measured at slow heating rates, Figure 3B), and the time course of the helix-to-coil transition was monitored by CD at 222 nm until steady state was attained (Figure 5, squares). Next, the temperature was lowered to 25 °C, and $[\Theta_{222}](t)$ was monitored during protein refolding (Figure 5, diamonds). These and other kinetic CD data recorded of apoC-1/DMPC complexes are well approximated by single exponentials, suggesting that the α-helical folding/unfolding can be approximated by a first order reaction (eq 1, Materials and Methods). Single-exponential data fitting indicate nearly 10-fold difference between the exponential relaxation times for the unfolding and refolding, $\tau_U = 35.5$ min and $\tau_R \sim 3.4$ min. Relatively fast refolding was also observed in T-jumps from higher temperatures (50−85 °C), which may explain the absence of scan rate dependence in the refolding data recorded at fast cooling rates (0.76−1.34 K/min, closed symbols in Figure 4A).

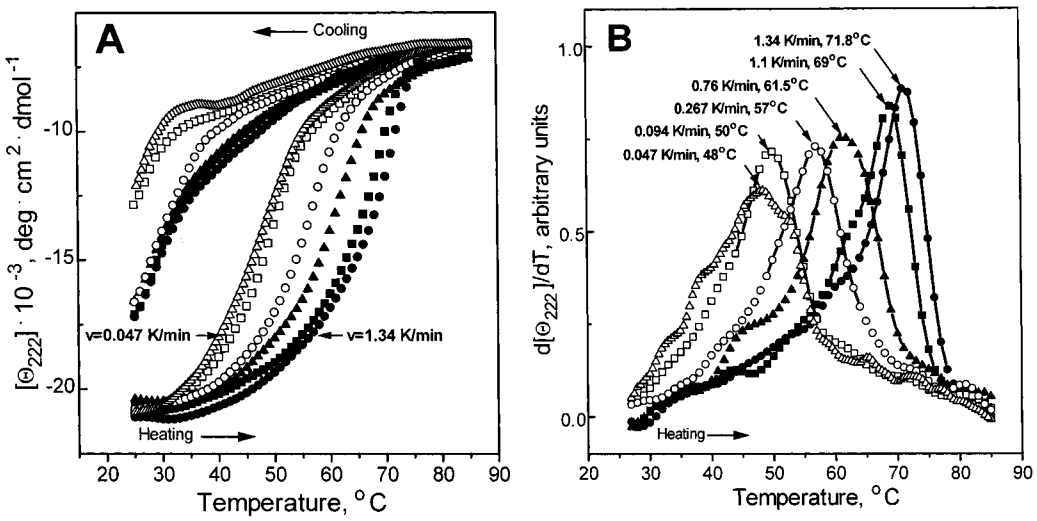

FIGURE 4: Scanning rate effects on the CD melting curves of apoC-1 in DMPC complexes. (A) Thermal unfolding and refolding curves $\Theta_{222}(T)$ recorded by CD at 222 nm upon heating and cooling from 25 to 85 °C at several constant scanning rates: ● − 1.34 K/min, ■ − 1.10 K/min, ▲ − 0.76 K/min, ○ − 0.27 K/min; □ − 0.094 K/min; △ − 0.047 K/min. (B) First derivative functions $d\Theta_{222}/dT$ of the heat unfolding curves. Peak positions at various scanning rates and the corresponding values of the apparent melting temperature T_m are indicated.

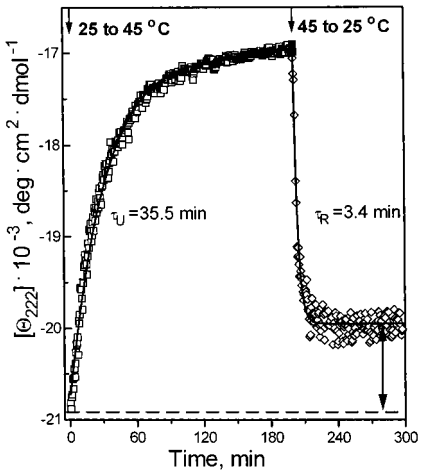

FIGURE 5: Kinetics of apoC-1 unfolding and refolding on DMPC disks monitored by far-UV CD in T-jump experiments from 25 to 45 °C. The disk solution was prepared as in Figure 2; the CD signal of this solution at 25 °C, $[\Theta_{222}](t) = \text{const}$, is shown by a horizontal line. The unfolding and refolding reactions were initiated by a T-jump from 25 to 45 °C (□) followed by a T-jump from 45 to 25 °C (◇). Short arrows show the starting times of the T-jumps. Double arrow indicates the loss in $[\Theta_{222}]$ after the heating and cooling to 45 °C. Solid lines show least-squares fitting of the data by single exponentials; the exponential relaxation times τ_U and τ_R for the unfolding and refolding directions are indicated. The reproducibility in the values of τ determined in repetitive experiments is better than 10%.

Protein refolding in apoC-1/DMPC complexes observed in T-jump experiments appears incomplete at any temperature explored. For example, the kinetic data in Figure 5 show that, after equilibration at 45 °C followed by equilibration at 25 °C, only ∼75% of the total loss in $[\Theta_{222}]$ is restored. Consequently, in contrast to free protein, the reduction in the CD amplitude at 25 °C observed after apoC-1/DMPC disk heating (Figures 3B and 4A) is not confined to high temperatures but occurs throughout the transition range. Incomplete CD recovery upon heating and cooling is also observed at other temperatures (50−85 °C) and other wavelengths (193 nm), suggesting reduced protein availability for the disk formation and/or a very slow kinetic step in the disk reconstitution. Regardless of the exact character of the transition (slowly reversible or partially irreversible), the mathematical treatment leading to determination of the energy barrier responsible for slow kinetics is similar (*42*).

Activation Enthalpy E_a and Free Energy ΔG^* for the ApoC-1 Unfolding on DMPC Disks. Slow transition kinetics depicted in Figure 5 indicates that the apoC-1/DMPC disk unfolding is associated with high Gibbs free energy barrier ΔG^*. The enthalpic contribution to this free energy barrier is well approximated by the Arrhenius activation energy E_a. The value of E_a was determined from the temperature dependence of the transition rate $k(T)$ measured in T-jumps from 25 °C to several constant temperatures from 40 to 85 °C. The time course of the reaction initiated by a T-jump was monitored by CD at 222 nm (Figure 6A). The $[\Theta_{222}](t)$ data are closely approximated by single exponentials (Figure 6A, solid lines). The exponential relaxation time τ that is inverse of the reaction rate, $\tau = 1/k$, is strongly temperature dependent and changes from >3 h at 40 °C to ∼90 s at 85 °C (Figure 6A). An Arrhenius plot ln k versus $1/T$ is linear (Figure 6B), suggesting that the unfolding follows Arrhenius law with $E_a(T) = \text{const}$ in the temperature range explored (eq 2, Materials and Methods). The slope of this plot yields the activation energy $E_a = 21 \pm 5$ kcal/mol.

An independent estimate of E_a was obtained from the analysis of the scan rate effect on the apparent melting temperature T_m (Figure 4B) using eq 3. This approach, which was originally derived for the kinetic analysis of irreversible unfolding monitored by DSC (*31*, *32*), assumes the first order reaction rate k that changes with temperature according to the Arrhenius law (eqs 1 and 2). The applicability of these assumptions to apoC-1 unfolding on the disks is suggested by the kinetic data in Figure 6A,B. We used eq 3 with T_m values taken at the peak temperatures in $d[\Theta_{222}](T)/dT$ functions recorded at various heating rates (Figure 3B). The plot $\ln(v/T_m^2)$ versus $(1/T)$ is linear (Figure 7), suggesting that $E_a(T) = \text{const}$ in the range of observed T_m. The slope of this plot yields the activation energy $E_a = 25 \pm 5$ kcal/mol; a comparable value of $E_a = 23 \pm 5$ kcal/mol is obtained from a similar plot by using the values of $T_{1/2}$ instead of

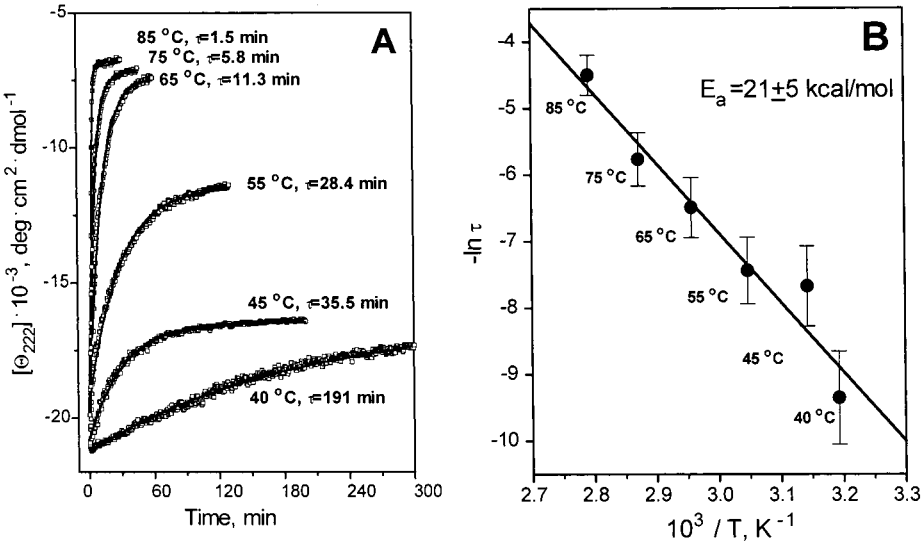

FIGURE 6: Kinetics of the apoC-1 unfolding on DMPC disks monitored in T-jumps from 25 to 85 °C. (A) CD data $\Theta_{222}(t)$ recorded in T-jumps from 25 °C to 40−85 °C; the final temperatures are indicated. Sample conditions are as in Figure 2. Solid lines show least-squares fitting of the data by single exponentials; the exponential relaxation times τ are indicated. (B) Arrhenius plot ln k versus $1/T$ for apoC-1 unfolding on the DMPC disks. Abscissa represents the final sample temperature after the T-jump (the values of T are indicated on the data), ordinate represents the reaction rate $k(T) = 1/\tau(T)$. Error bars correspond to the uncertainty in the determination of τ. Solid line shows least-squares data fitting by a linear function; the energy barrier determined from the slope of this function is $E_a = 21 \pm 5$ kcal/mol. The error in E_a incorporates the fitting errors and the uncertainty in the determination of τ.

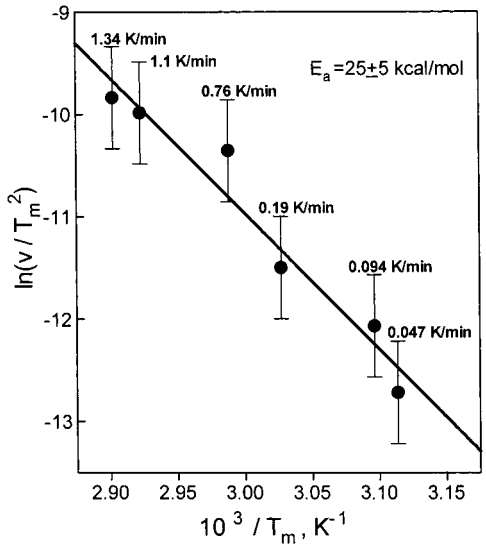

FIGURE 7: Energy barrier E_a determined from the heating rate effects on the apparent melting temperature T_m. Abscissa represents the values of T_m obtained from differentiation of the CD melting curves recorded at various scanning rates υ (Figure 4). The error bars represent uncertainty in the determination of T_m. Solid line shows least-squares fitting of the data by a linear function; the energy barrier determined from the slope of this function is $E_a = 25 \pm 5$ kcal/mol; the error incorporates the uncertainty in T_m determination and the fitting errors.

T_m. Agreement with the value of $E_a = 21 \pm 5$ kcal/mol determined from the Arrhenius plot confirms the validity of our kinetic analysis.

The value of ΔG^* can be determined from the reaction rate k using Eyring equation (eq 4, Materials and Methods) (*31*, *32*). Using the values of $k = 1/\tau$ measured in T-jump experiments (Figures 5 and 6A) with the standard rate equation with prefactor $k_B T/h \sim 6-7 \times 10^{12}$ s^{-1} yields the free energy barrier of $\Delta G^* = 24 \pm 0.5$ kcal/mol that is nearly invariant from 40 to 85 °C. Using a more realistic prefactor of 10^8 s^{-1} that approximates the helical folding/unfolding rate in the absence of the barrier (*35*−*37*) yields the activation free energy $\Delta G^* = 17.3-16.3$ kcal/mol at 40−85 °C; extrapolation to 25 °C suggests $\Delta G^* \sim 17-18$ kcal/mol for apoC-1 unfolding on DMPC disks.

Heat-Induced Changes in UV Light Scattering of ApoC-1/DMPC Complexes. In addition to measuring CD, the spectropolarimeter also registers high voltage applied to the dynodes of the UV detector photomultiplier (dynode voltage, V). Dynode voltage increases nearly linearly with the reduction in the light intensity that may result from light scattering and/or absorption. Since the extinction coefficient is weakly temperature dependent, no significant variations in UV absorption are expected to occur in the melting or kinetic CD experiments depicted in Figures 3B and 4A or 6A; indeed, the dynode voltage $V_{222}(T)$ at 222 nm is invariant upon heating and cooling lipid-free protein solution from 25 to 85 °C (Figure 8, insert). Consequently, any temperature-dependent variations in $V_{222}(T)$ of apoC-1/DMPC complexes must originate from the changes in the light scattering of these complexes.

The intensity of the scattered light depends on the refractive index of the particles and their radii and increases sharply as the particle size approaches the wavelength of light. Thus, UV light scattering ($\lambda \sim 200$ nm) of apoC-1/DMPC complexes ($d \sim 20$ nm) may significantly contribute to the dynode voltage, especially at higher temperatures when the particle diameter increases (Figure 1). Therefore, changes in $V_{222}(T)$ can be used to monitor heat-induced changes in the size and/or refractive index of the apoC-1/DMPC complexes.

The advantage of simultaneously measuring $V_{222}(T)$ and $\Theta_{222}(T)$ data is the increased accuracy of correlating the light scattering and the CD data. This is illustrated in Figure 8A that shows $V_{222}(T)$ data recorded at several scanning rates in the same series of experiments as the CD melting curves $\Theta_{222}(T)$ in Figure 4A. The $V_{222}(T)$ data show that heating from 25 to 85 °C leads to an increase in the dynode voltage,

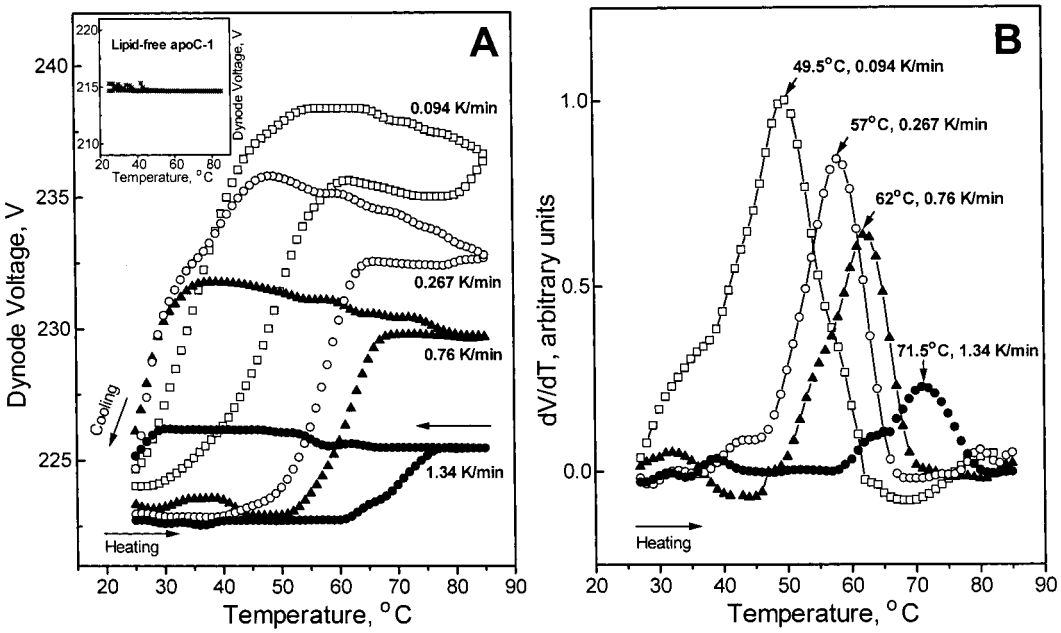

FIGURE 8: Scanning rate effects on the dynode voltage melting curves $V_{222}(T)$ of apoC-1/DMPC complexes. (A) Dynode voltage data recorded at 222 nm upon heating and cooling from 25 to 85 °C at several constant scanning rates. Data were recorded in the same series of CD experiments as the $\Theta_{222}(T)$ data in Figure 4. Line coding is same as in Figure 4; scanning rates are indicated on the lines. Incremental changes in the shallow portions of the curves result from imperfect analog-to-digital signal conversion. Inset: Dynode voltage data $V_{222}(T)$ recorded upon heating and cooling lipid-free apoC-1; sample conditions are same as in Figure 2. (B) First derivative functions dV_{222}/dT of the dynode voltage heating curves. The peak positions and the corresponding heating rates are indicated.

suggesting an increase in the particle size (i.e., disk-to-vesicle fusion) and/or refractive index (that may reflect formation of multilamellar vesicles). In contrast to the pre- and post-transitional CD values that are independent of the scanning rate (Figure 4A), the dynode voltage data show a progressive increase in the post-transitional values upon reduction in the scanning rate from 1.34 to 0.094 K/min (Figure 8A). This suggests that slower heating, i.e., prolonged sample exposure to elevated temperatures, leads to the formation of larger and/or multilamellar vesicles. Reduced lipid accessibility in such large multilamellar vesicles may result in slower kinetics of the disk reassembly upon cooling, leading to anomalous CD cooling curves observed at slow heating rates (Figure 4A, open symbols). The absence of any detectable effect of the increase in the particle size on the CD signal at high temperatures (Figure 4A) is consistent with the absence of any significant absorption flattening or differential light scattering effects in our CD experiments.

Similar to $\Theta_{222}(T)$ curves, the $V_{222}(T)$ curves clearly show hysteresis and scan rate effects on T_m, indicating nonequilibrium heat-induced morphological changes in apoC-1/DMPC complexes. Notably, the peak temperatures T_m in the first derivative functions $d[\Theta_{222}]/dT$ and dV_{222}/dT agree to better than 1 °C (Figure 4B and 8B), that is, within the accuracy of their experimental estimate; consequently, the activation energies for the heat-induced protein unfolding and particle transformation are identical. This remarkable agreement indicates that the heat-induced α-helical unfolding in apoC-1/DMPC complexes is closely coupled with the concomitant change in the particle morphology (particle fusion).

Scan rate effects on the $V_{222}(T)$ data in the post-transitional regions of the heating curves and in the cooling curves in Figure 8A are more complex. At $\upsilon = 1.34$ K/min, $V_{222}(T) =$ const upon heating and consecutive cooling from 75 to 85 °C but shows a small increase upon further cooling below 60 °C followed by a reduction below 30 °C (Figure 8A, solid circles) that may reflect disk reconstitution from larger vesicles. At slower scanning rates, progressive deviations between the heating and cooling curves in the post-transitional region and increases in $V_{222}(T)$ in the high-temperature portions of the cooling curves are observed, suggesting continued increase in the particle size and/or refractive index upon prolonged exposure to high temperatures. In all experiments, the dynode voltage $V_{222}(25\ °C)$ measured after heating and cooling from 25 to 85 °C shows a small but significant increase by 2−3 V compared to its pretransitional value, suggesting a small increase in the particle size and/or lamellar structure. This agrees with the small increase in the disk diameter observed in these samples by electron microscopy (Figure 1A,D).

Near-UV CD and Trp Fluorescence. To characterize changes in the environment of a single Trp41 in apoC-1 that may accompany DMPC binding, intrinsic Trp fluorescence and near-UV CD spectra were recorded of free protein and of apoC-1/DMPC disk solutions (Figure 9). Comparison of the fluorescence spectra recorded at 25 °C from freshly prepared solutions of free apoC-1 monomer and of apoC-1/DMPC disks (solid and dotted lines in Figure 9) shows that the disk formation leads to an increase in the spectral intensity and a blue shift in the wavelength of maximal fluorescence from 355 to 333 nm, indicating reduced solvent accessibility of Trp41 side chain and reduced polarity in its environment. In contrast, near-UV CD spectra of apoC-1 at 25 °C (Figure 9, inset) show no large changes upon DMPC binding, indicating the absence of any significant changes in the asymmetry of the environment of Trp41; to our knowledge, this is the first report on an apolipoprotein with near-UV CD that is invariant upon lipid binding. Consequently, apoC-1/DMPC disk formation shields Trp41 side

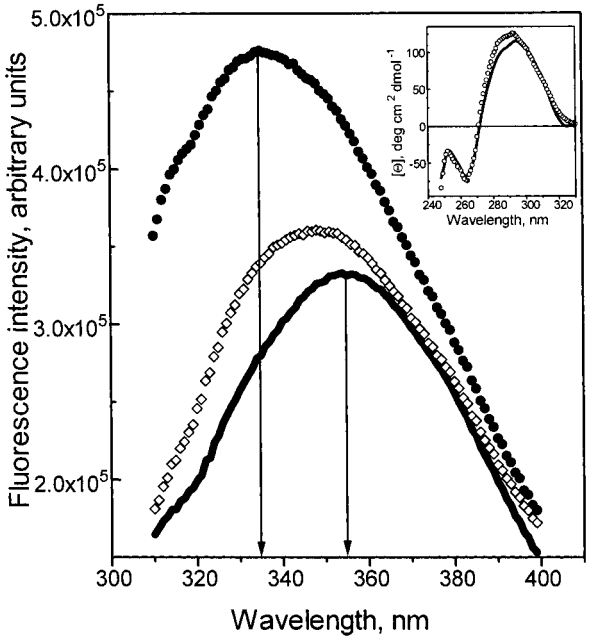

FIGURE 9: Effects of DMPC binding on Trp fluorescence and near-UV CD spectra of apoC-1. Intrinsic Trp fluorescence spectra (excitation wavelength, 290 nm) were recorded at 25 °C of free apoC-1 (−), freshly prepared apoC-1/DMPC disks (●), and similar disks that were equilibrated for 1 h at 65 °C followed by 20 min equilibration at 25 °C (◊). Protein concentration in all samples is 5 μg/mL. Arrows indicate the wavelength of maximal fluorescence. Inset: Near-UV CD spectra of free apoC-1 (−) and apoC-1/DMPC complexes (○) at 25 °C. No large changes in near-UV CD were detected after sample equilibration at 75 °C (data not shown to avoid overlap).

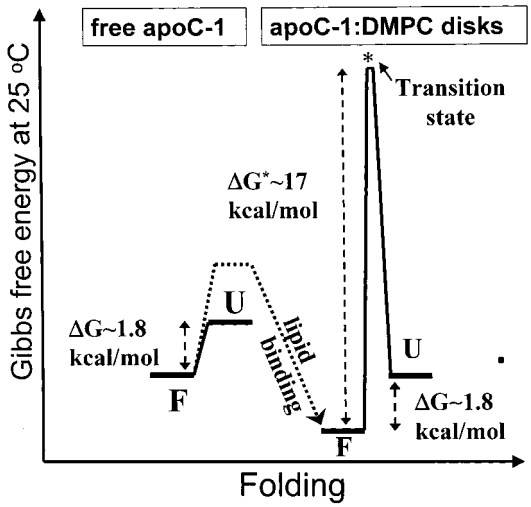

FIGURE 10: Free energy diagram of lipid-free and DMPC-bound apoC-1. The apparent thermodynamic stability of apoC-1/DMPC disks is comparable to that of free apoC-1, $\Delta G \sim 1.8$ kcal/mol, and is about an order of magnitude lower than the free energy barrier separating the folded (F) and unfolded (U) states of the protein on the DMPC complexes, $\Delta G^* \geq 17$ kcal/mol. High free energy of the transition state (indicated by *) accounts for the rate-limiting step F → * in the F→ * → U lipoprotein transition. Lipid binding (indicated by dotted arrow) is driven by a reduction in the free energy G_F of the folded state of the system containing protein, lipid and buffer. Since the free energy of the unfolded state G_U is also likely to be lower for the lipid-bound protein, the thermodynamic stability of the system $\Delta G = G_U - G_F$ may not necessary increase upon lipid binding.

chain from the solvent but induces no conformational changes in this or adjacent groups. This result is consistent with our earlier near-UV CD studies showing that the packing of the hydrophobic cluster containing Trp41 is conserved in the broad range of environmental conditions (the α-helical content under these conditions varies from 5 to 75%) and suggesting that this cluster forms the most stable helical element in apoC-1 (*18*).

Near-UV CD spectra of apoC-1/DMPC complexes, similar to those of free apoC-1 (*18*), do not significantly change in the temperature range 25−85 °C, indicating that the packing of Trp 41 remains invariant upon α-helix unfolding in apoC-1 that occurs at these temperatures. In contrast, Trp fluorescence spectra of apoC-1/DMPC samples subjected to different thermal treatments are significantly different. For example, the fluorescence spectrum of a disk solution that was equilibrated for 1 h at 65 °C followed by ≥20 min equilibration at 25 °C (open symbols in Figure 9; the corresponding electron micrograph is shown in Figure 1C) appears intermediate between the spectra of free apoC-1 and of freshly prepared disk solution at 25 °C, providing an additional evidence for an irreversible (or very slowly reversible) step in the apoC-1 unfolding in complex with DMPC.

DISCUSSION

Our results demonstrate that the unfolding of apoC-1 moiety in DMPC complexes, in contrast to that of free apoC-1, is a slow nonequilibrium transition associated with high activation energy and enthalpy. This is evident from the marked hysteresis and the scan rate dependence in far-UV CD and dynode voltage melting curves of apoC-1/DMPC complexes (Figures 4 and 8), and from the slow temperature-dependent transition rate revealed in T-jump experiments (Figures 5 and 6). This nonequilibrium character of the apoC-1/DMPC transition, along with its intrinsic irreversibility or slow reversibility [suggested by a small increase in the disk diameter (Figure 1) and an incomplete recovery in the CD, dynode voltage and fluorescence signals upon heating and cooling from 25 °C to higher temperatures (Figures 3B, 4A, 5, and 9)], preclude quantitative thermodynamic analysis of this transition.

Qualitatively, similar to heat unfolding of free apoC-1 (Figure 3A), the unfolding of apoC-1 in DMPC disks at slow heating rates (Figure 4, open triangles) starts slightly above 25 °C, becomes significant at 37 °C, and has an apparent transition temperature $T_m = 48$ °C, close to $T_m = 51$ °C of free apoC-1 (*17*, *42*). Thus, disk formation with DMPC may not substantially increase the low thermodynamic stability of apoC-1 at these temperatures [at 25 °C, the apoC-1 stability was measured to be $\Delta G(25\ °C) \sim 1.8$ kcal/mol (*43*)]. Similarly, chemical unfolding studies of small discoidal or spherical HDL containing apoA-1 and various amounts of phospholipid and cholesterol suggest that the protein thermodynamic stability does not necessarily increase upon lipidation (*5*, *19*, *21*, *22*, *44*). These results exemplify that spontaneous protein−lipid association is driven by a reduction in the free energy G_F of the system containing folded protein, lipid, and buffer, and may not necessarily be accompanied by an increase in the thermodynamic stability $\Delta G = G_U - G_F$ of this system (Figure 10).

In summary, our results corroborate earlier data indicating irreversible kinetically controlled unfolding of apoA-1/

DMPC disks (*23*, *26*, *27*) and suggest that the unfolding of other PC-containing reconstituted lipoproteins may also be a subject of the kinetic control. Indeed, the size and stoichiometry of the reconstituted lipoproteins depend not only on the environmental conditions and the protein/lipid ratio, but also on the temperature and the physical state of lipid at the time of the reaction [gel or liquid crystalline, single or multilamellar vesicles, (*10* and references therein)], suggesting that the reaction products are kinetically trapped. Furthermore, both reconstituted and, especially, plasma lipoproteins are compositionally and structurally heterogeneous complexes lacking the packing specificity that is thought to account for the stability of tightly packed globular proteins (*45*). It therefore is likely that the mechanism of lipoprotein stabilization differs from the thermodynamic stabilization of globular proteins. We hypothesize that, similar to reconstituted DMPC-containing lipoprotein disks, nascent HDL (that also contain PCs as their major lipid constituents) may also be stabilized by kinetic rather than thermodynamic factors.

How can lipoproteins maintain their functional state despite their marginal thermodynamic stability? The answer is suggested by the slow kinetics of apolipoprotein unfolding on lipoproteins that occurs on a much longer time scale (minutes to hours, Figure 6) as compared to folding−unfolding transitions in small helical proteins (nano- to milliseconds). Such a slow transition kinetics suggests that the population distribution between the "folded" and "unfolded" lipoprotein species is determined not by their free energy difference ΔG but by the free energy barrier ΔG^* separating these species. Using standard rate equation sets the upper limit for ΔG^* at ~24 kcal/mol; a similar value of $\Delta G^* \sim 25$ kcal/mol was determined from the kinetic analysis of apoA-1/DMPC disk unfolding (*27*). Using the rate equation with a more realistic prefactor of 10^8 s^{-1} yields the value of $\Delta G^*(25\ °C) \sim 17-18$ kcal/mol. These estimates clearly demonstrate that the free energy barrier for the apoC-1/DMPC disk melting, $\Delta G^* \geq 17$ kcal/mol, is about an order of magnitude higher than the apparent thermodynamic stability, $\Delta G < 2$ kcal/mol (Figure 10). This indicates kinetic rather than thermodynamic mechanism for the disk stabilization.

The marked temperature dependence of the transition rate (Figure 6) indicates that the kinetic barrier for the apoC-1/DMPC disk disruption has a large enthalpic component ΔH^*. We used two independent experimental approaches to estimate Arrhenius activation energy E_a that approximates ΔH^*. The value of $E_a \sim 25 \pm 5$ kcal/mol determined from the scan rate effect on the apparent melting temperature T_m agrees with the value of $E_a \sim 21 \pm 5$ kcal/mol obtained from the Arrhenius analysis of the kinetic data (Figures 6 and 7). Comparison of these values with Gibbs free energy of activation, $\Delta G^* = \Delta H^* - T\Delta S^* \geq 17$ kcal/mol, indicates that the free energy barrier is dominated by enthalpy. This implies that the free energy barrier for the apoC-1 unfolding on DMPC disks originates mainly from the transient disruption of atomic packing interactions, rather than from the transient solvent exposure of apolar groups. Furthermore, the height of the energy barrier that defines kinetic lipoprotein stability is determined by the molecular nature of both the "folded" and the "transition" states (Figure 10). Thus, in addition to the molecular models of discoidal lipoproteins such as nascent HDL that are currently being developed (reviewed in refs *9* and *45*), the structure of the transition state will have to be addressed in detail to elucidate the molecular origin of lipoprotein stability.

The physical origin of the enthalpic barrier for the protein unfolding in complex with lipid is suggested by the correlation between the CD data $\Theta_{222}(T)$ that report on α-helix unfolding and the dynode voltage data $V_{222}(T)$ that report on changes in the morphology of apoC-1/DMPC complexes. The remarkable agreement between the apparent T_m values in the CD and light scattering melting curves (Figures 4B and 8B) indicates close coupling between the microscopic event, that is the unfolding of the protein moiety, and the macroscopic event, that is the heat-induced increase in the particle size and/or lamellar structure. This coupling suggests that the energy barrier for the apoC-1 unfolding on the disks (but not in lipid-free state) arises from the transient disruption of lipid−protein and/or lipid−lipid packing interactions upon the heat-induced protein unfolding and concomitant particle fusion.

The results of this work, together with the earlier studies (*23*, *27*, *28*), and our ongoing studies of DMPC complexes with human apoA-1 and its fragments (Yang Chao, Yiling Fang, O. G., and David Atkinson, unpublished data) suggest that the kinetic mechanism provides a general strategy for stabilization of discoidal lipoproteins that have PCs as their major lipid component. High kinetic barrier prevents such lipoproteins from fluctuating between the folded and unfolded states, which would otherwise result from their low thermodynamic stability. Comparison of the free energy of activation, $\Delta G^* \geq 17$ kcal/mol, determined for the unfolding of apoC-1 or apoA-1 on DMPC disks, with the free energy of stability of typical globular proteins, $\Delta G(25\ °C) = 11-16$ kcal/mol, shows that even though lipoproteins lack the high packing specificity that is thought to account for the globular protein stability (*46*), their kinetic stability may be comparable to the thermodynamic stability of globular proteins.

Kinetic stabilization has emerged as an important mechanism controlling folding and function of an increasing number of globular proteins (*47*−*49* and references therein), prion proteins (*50*), protein−DNA complexes (*51*), and was proposed to provide a general mechanism for stabilizing complex protein systems (*52*). We propose that lipoproteins represent another class of macromolecular complexes that are stabilized by kinetic factors. We suggest that such a kinetic mechanism of stabilization may have important implications for lipoprotein functions. It may not only maintain the stability of these heterogeneous complexes in the absence of high packing specificity, but may also enable lipoproteins to undergo multiple rounds of enzyme-regulated compositional and structural changes in the course of their metabolism independent of the effects of these changes on the thermodynamic stability. Kinetic barriers may also control the rates of apolipoprotein transfer among lipoproteins in the course of their metabolism.

ACKNOWLEDGMENT

We are indebted to Dr. David Atkinson for extremely helpful advice, discussions, and critical reading of the manuscript, and to Yang Chao and Yiling Fang for many useful discussions.

REFERENCES

1. Mahley, R. W., Innerarity, T. L., Rall, S. C., and Weisgraber, K. H. (1984) Plasma lipoproteins: apolipoprotein structure and function. *J. Lipid Res. 25*(*12*), 1277−1294.
2. Atkinson, D., and Small, D. M. (1986) Recombinant lipoproteins: implications for structure and assembly of native lipoproteins. *Annu. Rev. Biophys. Biophys. Chem. 15*, 403−456.
3. Eisenberg, S. (1990) Metabolism of apolipoproteins and lipoproteins. *Curr. Opin. Lipidol. 1*, 205−215.
4. Ginsberg, H. N. (1998) Lipoprotein physiology. *Endocrinol. Metab. Clin. North Am. 27*, 503−519.
5. Sparks D. L., Frank, P. G., Braschi, S., Neville, T. A.-M., and Marcel, Y. L. (1999) Effect of apolipoprotein A-1 lipidation on the formation and function of pre-β and α-migrating LpA-I particles. *Biochemistry 38*, 1727−1735.
6. Aggerbeck, L. P., Wetterau, J. R., Weisgraber K. H., Wu, C.-H. C., and Lindgren, F. T. (1988) Human apolipoprotein E in aqueous solution. II. Properties of the amino- and carboxy-terminal domains. *J. Biol. Chem. 263*, 6249−6258.
7. Gursky, O., and Atkinson, D. (1996) Thermal unfolding of human high-density apolipoprotein A-1: Implications for a lipid-free molten globular state. *Proc. Natl. Acad. Sci. U.S.A. 93*, 2991−2995.
8. Soulages, J. L., and Bendavid, O. J. (1998) The lipid binding activity of the exchangeable apolipoprotein apolipophorin-III correlates with the formation of a partially folded conformation. *Biochemistry 37*, 10203−10210.
9. Brouillette, C. G., Anantharamaiah, G. M., Engler, J. A., and Borhani, D. W. (2001) Structural models of human apolipoprotein A−I: A critical analysis and review. *Biochim. Biophys. Acta 1531*, 4−46.
10. Jonas A. (1986) Reconstitution of high-density lipoproteins. *Methods Enzymol. 128*, 553−582.
11. Segrest, J. P., Jones, M. K., De Loof, H., Brouillette, C. G., Venkatachalapathi, Y. V., and Anantharamaiah, G. M. (1992) The amphipathic helix in the exchangeable apolipoproteins: A review of secondary structure and function. *J. Lipid Res. 33*, 141−166.
12. Osborne, J. C. Jr., Lee, N. S., and Powell, G. M. (1986) Solution properties of apolipoproteins. *Methods Enzymol. 128*, 375−387.
13. Steyrer, E., and Kostner, G. M. (1988) Activation of lecithin-cholesterol acyltransferase by apolipoprotein D: comparison of proteoliposomes containing apolipoprotein D, A-I or C-I. *Biochim. Biophys. Acta 958*, 484−491.
14. Sehayek, E., and Eisenberg, S. (1991) Mechanisms of inhibition by apolipoprotein C of apolipoprotein E-dependent cellular metabolism of human triglyceride-rich lipoproteins through the low-density lipoprotein receptor pathway. *J. Biol. Chem. 266*, 18259−18267.
15. Swaney, J. B., and Weisgraber, K. H. (1994) Effect of apolipoprotein C-I peptides on the apolipoprotein E content and receptor-binding properties of beta-migrating very low-density lipoproteins. *J. Lipid Res. 35*, 134−142.
16. Rozek, A., Sparrow, J. T., Weisgraber, K. H., and Cushley, R. J. (1999) Conformation of human apolipoprotein C-I in a lipid-mimetic environment determined by CD and NMR spectroscopy. *Biochemistry 38*, 14475−14484.
17. Gursky, O. (1999) Probing the conformation of a human apolipoprotein C-1 by amino acid substitutions and trimethylamine-*N*-oxide. *Protein Sci. 8*, 2055−2064.
18. Gursky, O. (2001) Solution conformation of human apolipoprotein C-1 inferred from proline mutagenesis: Far and near-UV CD study. *Biochemistry 40*, 12178−12185.
19. Cho, K.-H., Durbin, D. M., and Jonas, A. (2001) Role of individual amino acids of apolipoprotein A−I in the activation of lecithin: cholesterol acyltransferase and in HDL rearrangements. *J. Lipid Res. 42*, 379−389.
20. Massey, J. B., and Pownall, H. J. (1986) Thermodynamics of apolipoprotein-phospholipid association. *Methods Enzymol. 128*, 403−413.
21. Sparks D. L., Lund-Katz S., and Phillips M. C. (1992) The charge and structural stability of apolipoprotein A-1 in discoidal and spherical recombinant high-density lipoprotein particles. *J. Biol. Chem. 267*, 25839−25847.
22. Sparks D. L., Davidson W. S., Lund-Katz S., and Phillips, M. C. (1995) Effects of the neutral lipid content of high-density lipoprotein on apolipoprotein A-I structure and particle stability. *J. Biol. Chem. 270*, 26910−26917.
23. Reijngoud, D.-J., and Phillips, M. C. (1982) Mechanism of dissociation of human apolipoprotein A-1 from complexes with DMPC as studied by guanidine hydrochloride denaturation. *Biochemistry 21*, 2969−2976.
24. Tall, A. R., Small, D. M., Deckelbaum, R. J., and Shipley, G. G. (1977) Structure and thermodynamic properties of high-density lipoprotein recombinants. *J. Biol. Chem. 252*, 4701−4711.
25. Parks, J. S., Atkinson, D., Small, D. M., and Rudel, L. L. (1981) Physical characterization of lymph chylomicra and very low-density lipoproteins from nonhuman primates fed saturated dietary fat. *J. Biol. Chem. 256*, 12992−12999.
26. Suurkuusk, M., and Singh, S. K. (2000) Formation of HDL-like complexes from apolipoprotein A-I_m and DMPC. *Intern. J. Pharmacol. 194*, 21−38.
27. Epand, R. M. (1982) The apparent preferential interactions of human plasma high-density apolipoprotein A-1 with gel-state phospholipids. *Biophys. Biochem. Acta 712*, 146−151.
28. Surewicz, W. K., Epand, R. M., Pownall, H. J., and Hui, S.-W. (1986) Human apolipoprotein A-I forms thermally stable complexes with anionic but not with zwitterionic phospholipids. *J. Biol. Chem. 34*, 16191−16197.
29. Huxley, H. E., and Zubay, G. (1960) Electron microscope observations on the structure of microsomal particles of *E. coli*. *J. Mol. Biol. 2*, 10−18.
30. John, D. M., and Weeks, K. M. (2000) Van't Hoff enthalpies without baselines. *Protein Sci. 9*, 1416−1419.
31. Sanchez-Ruiz, J. M., Lopez-Lacomba, J. L., Cortijo, M., and Mateo, P. L. (1988) Differential scanning calorimetry of irreversible thermal denaturation of thermolysin. *Biochemistry 27*, 1648−1652.
32. Sanchez-Ruiz, J. M. (1992) Theoretical analysis of Lumry-Eyring model in differential scanning calorimetry. *Biophys. J. 61*, 921−935.
33. Glasstone, S., Laidler, K. J., and Eyring, H. (1941) *The Theory of Rate Processes*, McGraw-Hill, New York.
34. Fersht, A. (1985) *Enzyme Structure and Mechanism*; Freeman, New York.
35. Gilmanshin, R., William, S., Callender, R. H., Woodruff, W. H., and Dyer, R. B. (1997) Fast events in protein folding: Relaxation dynamics of secondary and tertiary structure in native apomyoglobin. *Proc. Natl. Acad. Sci. U.S.A. 94*, 3709−3713.
36. d'Avignon, D. A., Bretthorst, G. L., Holtzer, M. E., and Holtzer, A. (1999) Thermodynamics and kinetics of a folded-folded transition at valine-9 of a GCN4-like leucine zipper. *Biophys. J. 76*, 2752−2759.
37. Crane, J. C., Koepf, E. K., Kelly, J. W., and Gruebele, M. (2000) Mapping the transition state of the WW domain β-sheet. *J. Mol. Biol. 298*, 283−292.
38. Forte, T. M., Nichols, A. V., Gong, E. L., Lux, S. and Levy, R. I. (1971) Electron microscopic study on reassembly of plasma high-density apolipoprotein with various lipids. *Biochim. Biophys. Acta 248*, 381−386.
39. Mao, D., and Wallace, B. A. (1984) Differential light scattering and absorption flattening effects are minimal in the circular dichroism spectra of small unilamellar vesicles. *Biochemistry 23*, 2667−2673.
40. Carra J. H., Anderson E. A., Privalov P. L. (1994) Thermodynamics of staphylococcal nuclease denaturation. I. Acid-denatured state. *Protein Sci. 3*, 944−951.
41. Leeson, D. T., Gai, F., Rodriguez, H. M., Gregoret, L. M., and Dyer R. B. (2000) Protein folding and unfolding on a complex energy landscape. *Proc. Natl. Acad. Sci. U.S.A. 97*, 2527−2532.

42. Potekhin, S. A., Loseva, O. I., Tiktopulo, E. I., and Dobritsa, A. P. (1999) Transition state of the rate-limiting step of heat denaturation of Cry3A δ-endotoxin. *Biochemistry 38*, 4121−4127.
43. Gursky, O., and Atkinson, D. (1998) Thermodynamic analysis of human plasma apolipoprotein C-1: high-temperature unfolding and low-temperature oligomer dissociation. *Biochemistry 37*, 1283−1291.
44. Parks J. S., and Gebre A. K. (1997) Long-chain polyunsaturated fatty acids in the sn-2 position of phosphatidycholine decrease the stability of recombinant high-density lipoprotein apolipoprotein A-1 and the activation energy of the lecithin:cholesterol acyltransferase reaction. *J. Lipid Res*. *38*, 266−275.
45. Narayanaswami, V., and Ryan, R. O. (2000) Molecular basis of exchangeable apolipoprotein function. *Biochim. Biophys. Acta 1483*(*1*), 5−36.
46. Privalov, P. L. (1989) Thermodynamic problems of protein structure. *Annu. Rev. Biophys. Biophys. Chem. 18*, 47−69.
47. Baker D., Agard D. A. (1994) Kinetics versus thermodynamics in protein folding. *Biochemistry 33*, 7505−7509.
48. Kobayashi, C., Suga, Y., Yamamoto, K., Yomo, T., Ogasahara, K., Yutani, K., and Urabe, I. (1997) Thermal conversion from low- to high-activity forms of catalase I from *Bacillus stearothermophilus*. *J. Biol. Chem*. *272*, 23011−23016.
49. Cunningham, E. L., Jaswal, S. S., Sohl, J. L., and Agard, D. A. (1999) Kinetic stability as a mechanism of protease longevity. *Proc. Natl. Acad. Sci. U.S.A. 96*, 11008−11014.
50. Baskakov, I. V., Legname, G., Pruisner, S. B., and Cohen, F. E. (2001) Folding of prion protein in its native α-helical conformation is under kinetic control. *J. Biol. Chem*. *276*, 19687−19690.
51. Cloutier, T. E., Librizzi, M. D., Mollah, A. K. M. M., Brenowitz, M., and Willis, I. M. (2001) Kinetic trapping of DNA by transcription factor IIIB. *Proc. Natl. Acad. Sci. U.S.A. 98*, 9581−9586.
52. Plaza del Pino, I. M., Ibarra-Molero, B., Sanchez-Ruiz, J. M. (2000) Lower kinetic limit to protein thermal stability: a proposal regarding protein stability in vivo and its relation with misfolding diseases. *Proteins 40*, 58−70.

BI025588W